National Seminar on Computational & Experimental Mechanics (CEM) 2005

Editors: *A. K. Ariffin, N. A. N. Mohamed, S. Abdullah and M. J. M. Nor*

NUMERICAL MODELING OF CYCLIC STRESS-STRAIN BEHAVIOR OF Sn-Pb SOLDER JOINT DURING THERMAL FATIGUE

M. N. Tamin and Y. B. Liew
Department of Applied Mechanics
Faculty of Mechanical Engineering
81310 UTM Skudai, JOHOR

ABSTRACT

This study examines the cyclic stress-strain response of solder joints in a surface mounted electronic assembly due to temperature cycles. For this purpose, a three-dimensional model of an electronic test package is analyzed using finite element method. The model consists of 92 solder joints arranged along the peripheral of a 24x24 solder array. The various different materials considered in the simulation are Si-die, 60Sn-40Pb solder alloy, Cu-traces, Cu_6Sn_5 intermetallics, FR-4 substrate and PCB. The temperature- and strain-rate-dependent plastic stress-strain curves define the viscoplastic response of the near-eutectic solder alloys. Orthotropic behavior of the FR-4 substrate and PCB is modeled. Other materials are assumed to behave elastically with temperature-dependent material properties. Temperature loading of the package consists of an initial cooling down from the re-flow temperature at 183 ^{o}C to 25 ^{o}C followed by thermal cycling between -40 to 125 ^{o}C. Results of the analysis show that the package warps with a magnitude of 93 μm at 25 ^{o}C after re-flow. In this process, the critical solder joint accumulated an inelastic strain of 0.856 percent. Faster temperature ramp rate at 370 ^{o}C/min (load case TR1) versus 33 ^{o}C/min (load case TC1) resulted in 12 percent lower inelastic strain after completing 3 temperature cycles. However, the inelastic strain magnitude is achieved in a much shorter time. The shear stress-strain hysteresis loops display the largest strain ranges compared to other stress-strain components. The calculated shear strain range is 0.8 percent with the corresponding stress range of 34.0 MPa.

Keywords: electronic packaging; solder joint; reliability; cyclic stress-strain behavior; finite element method

INTRODUCTION

In a surface mount electronic assembly, the electronic package is commonly attached to the printed circuit board (PCB) by solder joints. Temperature fluctuation due to device internal heat dissipation and ambient temperature changes generates thermo-mechanical loading on the assembly. Throughout the

loading, differential thermal expansion of the various component materials induces cyclic strains on the solder joints. These strains result in cumulative fatigue damage that could lead to premature fatigue failure of the joints. Thermal fatigue of solder joints, therefore, is critical to electronic package performance and reliability. The reliability of these solder joints is determined by the combined effects of component design, assembly design and use environment.

Temperature cycling of solder assemblies in an environmental chamber is intended to simulate the actual operating (power) cycles that consist of power on/off with or without ambient temperature changes. In this thermal cycling, the solder joint is subjected to cyclic stresses and strains beyond elastic limit of the solder alloy. Consequently, the stress-strain hysteresis loops dictate the accumulation of fatigue damage and determine the fatigue life of the solder joint. The failure mechanism, however, is complicated by the creep-fatigue interaction effect since the solder joint operates at high homologous temperature. At this temperature level, the solder alloy display significant rate dependent behavior.

Finite element modeling of electronic packages and PCB assembly has been widely employed to provide an insight to the understanding of failure mechanisms and long term reliability of solder joints in the assembly (Lau 1995, Lau and Yi-Hsin 1997). Its success lies in appropriate representation of the package geometry with associated boundary conditions and temperature loading, and the ability to accurately simulate the response of package materials during thermal cycling or shock. Consequently, accurate description of solder alloy behavior should account for both temperature and time-rate effects on the material as observed experimentally. For example, the tensile strength of eutectic Sn-Pb solder decreases from about 50 to 30 MPa following 60 days of thermal aging (Kishimoto et al. 2001). In addition, solder tensile properties can vary widely for different strain rates used in the tensile tests (Pang et al. 1998).

This paper investigates the cyclic stress-strain response of Sn-Pb solder joints connecting a test package to the PCB during re-flow and subsequent thermal cycles. Emphasis will be placed on the evolution characteristics and hysteresis cycles of stresses and strains, in relation to fatigue failure of the solder joint. The relative effects of temperature ramp rates on the mechanical response of the package are examined in terms of inelastic strain accumulation in the solder alloy.

FINITE ELEMENT MODELING

The finite element model of the test package consists of 92 solder joints arranged along the peripheral of a 24x24 solder array. The diameter, height and pitch distance of the solders is 760 μm, 600 μm and 1.0 mm, respectively. Due to symmetrical nature of the package, only one-quarter of the 3-D model is analyzed. An isometric and exploded views of the model is illustrated in Figure 1. The various different materials considered in the simulation are Si-die, near eutectic solder joints, Cu-traces, Cu_6Sn_5 intermetallics, FR-4 substrate and PCB. Thermal

analysis performed on the test package indicates that the transient effect is negligible, thus thermal boundary condition is not imposed in the stress analysis.

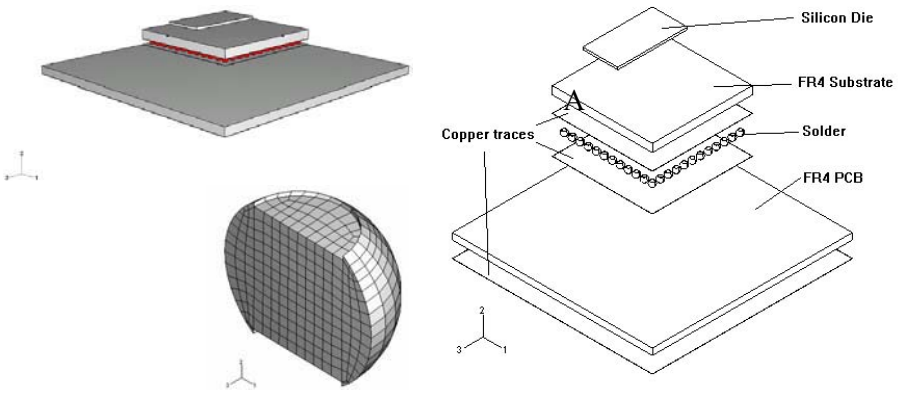

FIGURE 1 Isometric and Exploded View of the Test Package (Quarter Model). The Inset Figure Illustrates Mesh Size for the Cross-section View of a Solder Joint.

Temperature dependent material properties of Si, solder alloy, Cu-traces and FR-4 employed in the analysis are extracted from published literature (Adams 1986, Amagai 1999, Auersperg 1997, Pang et al. 2002). Strain-rate-dependent plastic stress-strain curves define the viscoplastic response of the 60Sn-40Pb solder alloys. Orthotropic behavior of FR-4 substrate and PCB is also modeled. Summary of the materials properties used in the simulation is shown in Figure 2 along with the stress-strain curves of the solder alloy at several test temperatures.

Material	Modulus of Elasticity, E (GPa) *T* in Kelvin	Poisson's Ratio, *v* *T* in Kelvin	CTE, α (ppm/ K) *T* in Kelvin
60Sn 40Pb (Adams, 1986)	$64.26 - 0.0718 * T$	$0.3244 + 1.1558\times10^{-4} * T$	21
Silicon (Shi *et al.*, 2002)	$132.46 - 0.00954\ T$	0.28	$2.113 + 0.00235\ T$
Copper (Shi *et al.*, 2002)	$141.92 - 0.0442\ T$	0.35	$15.64 + 0.0041\ T$
IMC Cu_6Sn_5 (Amagai, 1999a)	85.6	16.0	0.31

FR-4 (isotropic plane xy) (Auersperg, 1997)						
Properties	-40°C	30°C	95°C	125°C	150°C	270°C
Ex (MPa)	24252	22400	20680	19300	17920	16000
Ey (MPa)	24252	22400	20680	19300	17920	16000
Ez (MPa)	2031	1600	1200	1000	600	450
V_{xy}	0.02	0.02	0.02	0.02	0.02	0.02
V_{yz}	0.1425	0.1425	0.1425	0.1425	0.1425	0.1425
V_{xz}	0.1425	0.1425	0.1425	0.1425	0.1425	0.1425
α_x(ppm/°C)	16	16	16	16	16	16
α_y(ppm/°C)	16	16	16	16	16	16
α_z(ppm/°C)	65	65	65	65	65	65
Gxy (MPa)	662	630	600	500	450	441
Gxz (MPa)	210	199	189	167	142	139
Gyz (MPa)	210	199	189	167	142	139

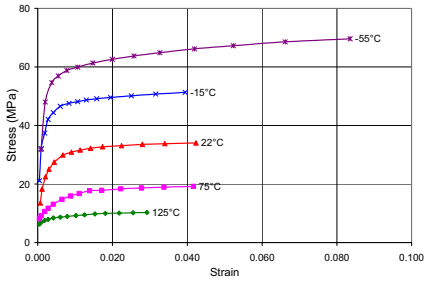

(a) (b)

FIGURE 2 (a) Properties of Various Materials Used in the Simulation. (b)Stress-Strain behavior of 60Sn-40Pb Solder Alloy at Strain Rate of $1.67\text{x}10^{-4}$ s^{-1}

Thermal loading of the test package, as illustrated in Figure 3, consists of an initial cooling down from re-flow temperature (183 ^{o}C) to room temperature, followed by thermal cycling between –40 to 125 ^{o}C. The effect of high temperature ramp rate (to simulate thermal shock stress) is examined by comparing two different load cases at 33 ^{o}C/min (TC1) and 370 ^{o}C/min (TR1)

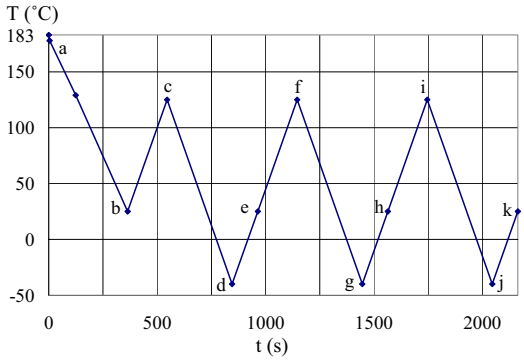

FIGURE 3 Temperature Loading Profile Consists of Re-flow Process (Path a-b) Followed by Temperature Cycles

RESULTS AND DISCUSSION

Re-flow Process (Cool-down)

Results of the finite element analysis show that the test package warps downward (with PCB on the bottom side) at room temperature (25 ^{o}C) with a magnitude of 93 μm following the re-flow process. At this temperature, the solder joint located at the symmetry line that is parallel with the longer side of the Si-die is the most critically strained solder (marked A in Figure 1). The evolution of von Mises stresses and the corresponding equivalent strains in this critical solder joint throughout the re-flow process is illustrated in Figure 4. It is noted that inelastic strains developed early following cooling down of the package from 183 ^{o}C. Although the stress level induced by coefficient of thermal expansion (CTE) mismatch is low, yield strength of the solder is also relatively low at high temperature. In addition, at this high homologous temperature, creep strain rate of the solder alloy is significant. Typical yield strength of 60Sn-40Pb solder alloys is 8 and 52 MPa at 125 and –55 ^{o}C, respectively when strained at 1.67×10^{-4} per second (Adams 1986). The stress is brought to the yield surface with the continuously accumulated inelastic strains. The von Mises stress reaches 24.0 MPa with the corresponding inelastic strain of 0.856 percent at room temperature.

In the critical solder joint, a high stress gradient develops along the interface between the solder and the Cu_6Sn_5 inter-metallic owing to both thermal expansion mismatches between the two materials and the severe geometric

discontinuities. Typical calculated Von Mises Stress and the corresponding equivalent inelastic

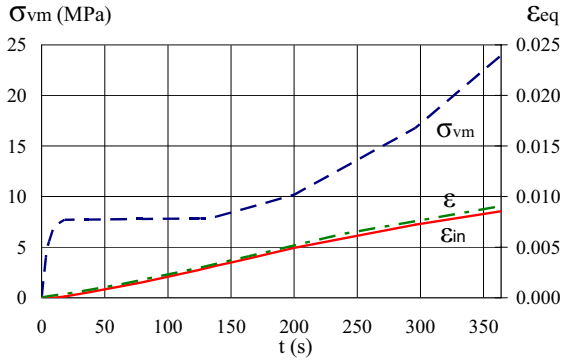

FIGURE 4 Evolution of Von Mises Stresses, Equivalent Total Strain and Equivalent Inelastic Strains in the Critical Solder During Re-flow Process.

strain distribution in the critical solder at 25 ^{o}C is shown in Figure 5. It is worth noting that the region of high stress occurs only to a small depth from the surface of the solder while the bulk of the solder remains elastic. The location underneath the edges of the chip (or intermetallic phase) is experiencing the maximum stress and strain hysteresis during subsequent thermal cycles. Consequently, extensive accumulation of cyclic inelastic strains in this locality is likely to initiate fatigue crack along the solder /intermetallic interfaces. Crack initiation in the solder corresponds to the location of the maximum creep and plastic strain (Sarihan 1999). In addition, solder fatigue cracking has been observed to initiate and propagate from similar location in chip scale packages (Amagai 1999, Lee et al. 1998). Catastrophic propagation of such crack is governed by fatigue and fracture parameters including stress level, fracture toughness and threshold stress intensity factor range.

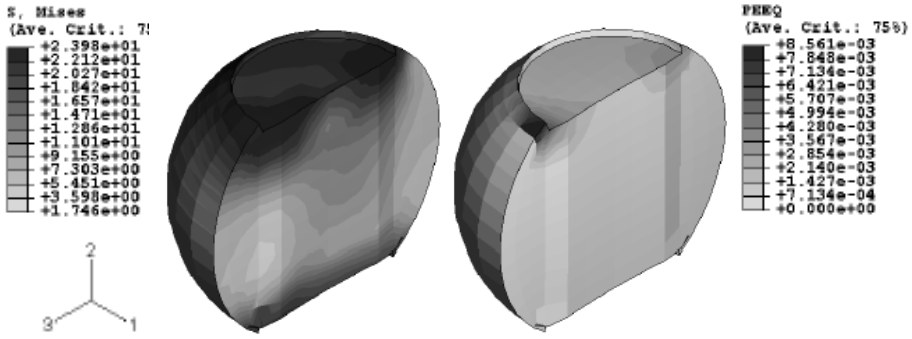

FIGURE 5 Von Mises Stress and Inelastic Strain Distribution in the Critical Solder Joint at 25 ^{o}C Following Re-flow Process (Cross-sectional View)

Thermal Cycles

The evolution characteristics of internal states in the critical solder joint during the application of temperature cycles are examined. Figure 6 compares the calculated inelastic strains in the critical solder joint for the two different heating and cooling rates. The heating and cooling rates for load case TR1 is 11.2 times faster than for load case TC1. Results show that, the accumulated inelastic strain for load case TR1 after completing 3 thermal cycles is about 12 percent lower than that for load case TC1. In the slow temperature cycling (TC1) longer time is spent at higher stress resulting in greater inelastic (creep) strain per cycle. However, the inelastic strain magnitude is achieved in much shorter time for thermal shock cycling (TR1). This result demonstrates the feasibility of employing thermal shock cycling as an alternative to temperature cycling in a reliability analysis on electronic packages for faster data turnaround.

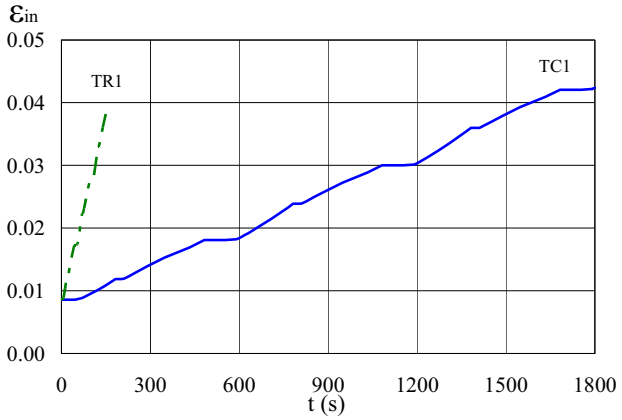

FIGURE 6 Effect of Temperature Ramp Rates on the Evolution of Inelastic Strain in the Critical Solder Joint After Completing 3 Thermal Cycles

The stress-strain hysteresis response of the solder alloy is examined in view of fatigue life prediction of solder joint. Figure 7 shows the hysteresis loops for all cartesian components of stresses and strains in the critical solder joint. The largest stress range is observed for the normal component (22-direction) with a magnitude of 78 MPa. The tensile part of this stress is favorable to Mode-I crack initiation at the solder/IMC interface layer. The shear component (23-direction) displays the largest strain range (at zero stress) of 0.8 percent with the corresponding shear stress range of 34.0 MPa. This large relative displacement within the solder /intermetallic interface attenuates the cyclic interfacial shear stress and strain resulting in crack initiation, as often observed experimentally. It is noted that although the shear stress range is larger (41.0 MPa) for faster temperature ramp rate (TR1), the resulting shear strain range is similar at 0.8 percent. For comparative purpose, a typical fatigue life of eutectic solder (with cycling frequency of 10 mins. /cycle) at a plastic strain range of 1.0 percent is about 5000 cycles (Hua et al. 1998). The hysteresis loop shifted towards larger

strain values following each temperature cycle indicating the continuous accumulation of inelastic strain.

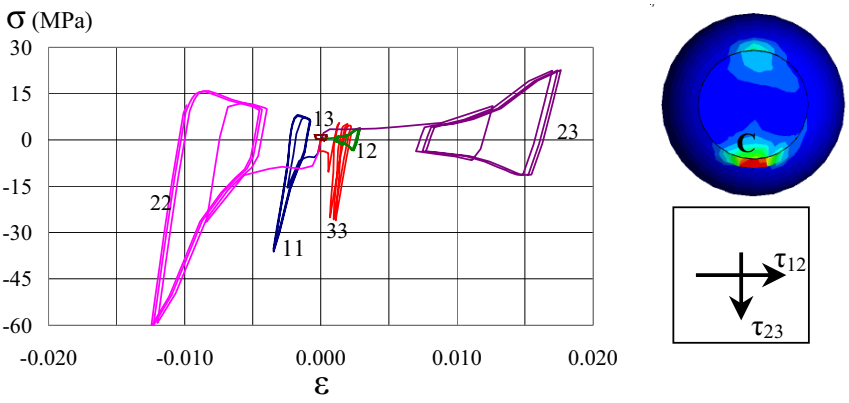

FIGURE 7 Stress-Strain Hysteresis Curves for the First Three Temperature Cycles of Load Case TC1. The Critical Yielded Material Point is Indicated as Point C. The Indices Denote the Six Cartesian Components

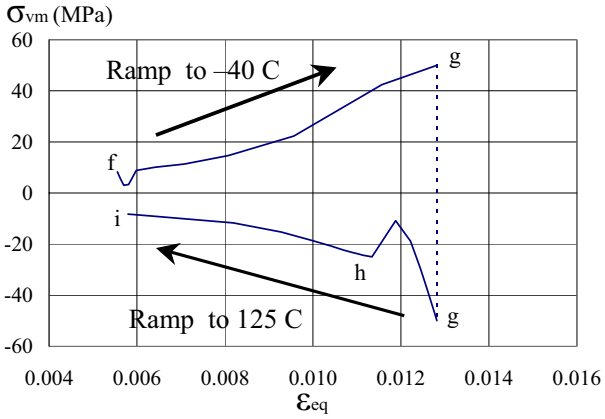

FIGURE 8 Equivalent Stress-Strain Hysteresis Loop for the 2nd Thermal Cycle Following Re-flow process.

The combined response of all cartesian cyclic stress and strain components is examined by plotting the hysteresis loop in terms of von Mises stress and equivalent strain. Figure 8 shows the hysteresis curve for the 2nd temperature cycle between –40 and 125 °C following the re-flow process (path f-g-h-i in Figure 3). In this figure, the sign of von Mises stress is assigned to be positive for decreasing temperature and negative for increasing temperature. The finite element results show that the stress and equivalent strain in the solder increase (50.2 MPa, 1.28 %) when the temperature is decreased from 125 to –40 °C (portion f-g). When the temperature is subsequently increased the stress relaxed

to 8.5 MPa while the corresponding equivalent strain decreased to 0.056 % (portion g-h-i). It is noted that during heating between –40 to 25 ^{o}C (path g-h), the stress components change sign, which is reflected in the inflection point along the hysteresis curve. This is the effect of bending induced by warpage of the package.

CONCLUSIONS

The cyclic stress-strain behavior of the Sn-Pb solder joint in a surface mount test package has been analyzed using finite element analysis. Results show that:

- The package warps downwards at 25 ^{o}C following the re-flow process with a magnitude of 93 μm. The induced inelastic strain is 0.856 percent. Additional inelastic strain of 3.5 percent is accumulated after 3 temperature cycles between -40 to 125 ^{o}C.
- Faster temperature ramp rate (370 versus 33 ^{o}C/min) accelerates the inelastic strain evolution per temperature cycle. However, the strain magnitude is 12 percent lower after three cycles.
- The stress-strain hysteresis curves show the largest normal component (22-direction) of the stress range with magnitude of 78 MPa. The shear component (23-direction) of the hysteresis loops displayed the largest strain range at 0.8 percent.

ACKNOWLEDGMENT

This work is supported by UTM-Intel Contract Research Grant (No. 68313).

REFERENCES

Adams P. J. 1986. Thermal Fatigue of Solder Joints in Micro-electronic Devices, *MS Thesis, Dept. Mech. Eng., MIT*, Cambridge, MA.

Amagai M. 1999. Chip Scale Package (CSP) Solder Joint Reliability and Modeling, *Microelectronics Reliability*, **39:** 463-477.

Auersperg J. 1997. Fracture and Damage Evaluation in Chip Scale Packages and Flip Chip Assemblies by FEA and Microdac, *ASME Symp. Applications of Fracture Mechanics in Electronic Packaging*, Dallas, Texas, pp. 133-138.

Hua F., Z. Mei & Glazer J. 1998. Eutectic Sn-Bi as an Alternative to Pb-Free Solder, *Proc. Electronic Components and Technology Conf.,* pp. 277-283.

Kishimoto K., Omiya M. & Amagai M. 2001. A mechanical reliability assessment of solder joints, *IEEE Symp. Electronic Materials and Packaging,* pp. 8-14.

Lau J. H. 1995. *Flip Chip Technologies*, New York: McGraw-Hill

Lau J. H. & Yi Hsin P. 1997. *Solder Joint Reliability of BGA, CSP, Flip Chip and Fine Pitch SMT Assemblies*, New York: McGraw-Hill,.

Lee T., Lee J. & Jung I. 1998. Finite element analysis for solder ball failures in chip scale package, *Microelectronics Reliability*, **38:** 1941-1947.

Pang H. L. J. 2002. A New Creep Constitutive Model for Eutectic Solder Alloy, *J. Electronic Packaging*, ASME, **124**: 85-90.

Pang H. L. J. 1998. Sensitivity study of temperature and strain rate dependent properties on solder joint fatigue life, *Proc. IEEE Electronic Packaging Technology Conference*, pp. 184-189.

Sarihan V. 1999. Temperature dependent viscoplastic simulation of controlled collapse solder joint under thermal cycling, *ASME Journal of Electronic Packaging,* **115**: 16-21.